Selectively Deuterated Liquid Crystalline Cyanoazobenzene Side-Chain Polyesters. 3. Investigations of Laser-Induced Segmental Mobility by Fourier Transform Infrared Spectroscopy

Christian Kulinna and Søren Hvilsted*

Condensed Matter Physics and Chemistry Department, Risø National Laboratory, DK-4000 Roskilde, Denmark

Claudia Hendann and Heinz W. Siesler

Department of Physical Chemistry, University of Essen, D-45117 Essen, Germany

P. S. Ramanujam

Optics and Fluid Dynamics Department, Risø National Laboratory, DK-4000 Roskilde, Denmark

Received July 1, 1997; Revised Manuscript Received January 22, 1998

ABSTRACT: The laser-induced anisotropy in thin films of an extensive number of cyanoazobenzene side-chain liquid crystalline polytetradecanedioates, -dodecanedioates, and -adipates selectively deuterated at different positions have been investigated with polarized FTIR spectroscopy. The analysis of the segmental orientation based on dichroic ratios of characteristic absorption bands shows that, in polyesters with long main-chain spacing (tetradecanedioates and dodecanedioates), not only the light sensitive azo chromophore but also the main-chain methylene segment and to a smaller extent the flexible spacer are preferentially oriented perpendicular to the laser light polarization. The extent of orientation increases with increasing spacer length. On the other hand, in the shorter adipates only the chromophore and the spacer are likewise oriented. Rapid-scan FTIR analysis performed on-line with the laser irradiation reveals that the alignment of the aliphatic segments arises simultaneously with the chromophore orientation. Temperature dependent infrared investigations of the laser-induced orientation shows that the preservation of the photoinduced anisotropy directly relates to the polyester phase behavior.

1. Introduction

Rewritable optical storage[1,2] is a relatively new technology attracting a lot of interest recently. High-density optical storage in polymer materials[3−5] is a promising area as the materials can be produced cheaply in large, commercial quantities. Especially, utilization of the photochromic properties of azobenzene[6] has attracted considerable attention since the light-induced *trans*−*cis*−*trans* isomerization cycles have been well studied in the literature. Different systems with azo dyes dispersed in polymers,[7,8] azobenzene side chains in unoriented amorphous,[9−11] or prealigned liquid crystalline polymers[12−16] have been proposed and investigated. Recently, we introduced a new, flexible, and modular cyanoazobenzene side-chain liquid crystalline polyester architecture.[17,18] Most prominently, unoriented thin films of these polytetradecanedioate polyesters have been shown to possess diffraction efficiencies of more than 60% in a polarization holographic setup. High-resolution gratings[19] (more than 5000 lines/mm) have been fabricated. Holograms made six years ago show no sign of decay.[18] The stored information can be erased by heating the films to about 80 °C and cooling to room temperature and the film can be reused.[20] The stored information can also be erased by light.[21]

The resulting photoinduced anisotropy in these polyester materials has been studied in detail by focusing on the dichroic behavior of the nitrile vibrational band employing polarized Fourier transform infrared (FTIR) spectroscopy.[22] Recently, it was also shown for the first time experimentally by use of optical and FTIR spectroscopy that a red laser beam at 633 nm causes *cis*−*trans* transitions in azobenzene side-chain polyesters.[23] So far, only absorption bands originating from the azobenzene chromophore have been accessible to the dichroic, spectroscopic FTIR analysis without interference. Since the different structural parameters inherently possible by the modular construction have been found to significantly influence the optical storage properties, it has long been speculated[24] that not only the photoaddressable azobenzene chromophore furnish the anisotropy but also other material segments could contribute to the final material anisotropy. Varying the flexible alkyl side-chain spacer linking the photochromic moiety to the main chain from hexyl to decyl significantly affects the storage dynamics.[25] On the other hand, a relatively short main-chain segment provided by adipate exhibits an interesting biphotonic behavior.[26,27] However, due to the chemical similarity of the other main constituents of the polyester system, the aliphatic flexible spacer and the main-chain segment are not distinguishable in a dichroic FTIR experiment. Consequently, a methodology enabling the study of fundamental segmental mobility was aimed at. The most pertinent and powerful molecular marking tool seems to be strategic proton exchange with deuteron. Chemically, several exchange possibilities are available and a spectroscopically large impact is to be expected.[28,29]

This paper presents the detailed segmental analysis of anisotropy induced by laser light in thin films of

* To whom correspondence should be addressed. E-mail: s.hvilsted@risoe.dk.

S0024-9297(97)00967-4 CCC: $15.00
Published on Web 03/20/1998

Table 1. Molecular Structure, Position of Selective Deuteration, and Notation of the Investigated Cyanoazobenzene Side-Chain Polyesters

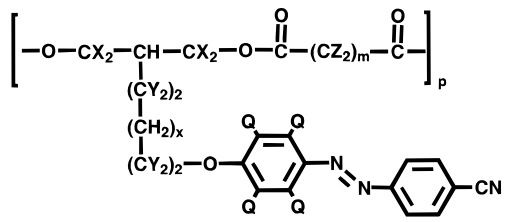

polyester	main-chain segment (***m***)	methylenes in spacer, ***n***[a]	X	Y	Z	Q
P6,12	tetradecanedioate (**12**)	**6**	**H**	**H**	**H**	**H**
P6,12X	tetradecanedioate (**12**)	**6**	**D**	**H**	**H**	**H**
P6,12Y	tetradecanedioate (**12**)	**6**	**H**	**D**	**H**	**H**
P6,12Z	tetradecanedioate (**12**)	**6**	**H**	**H**	**D**	**H**
P6,12XZ	tetradecanedioate (**12**)	**6**	**D**	**H**	**D**	**H**
P6,12Q	tetradecanedioate (**12**)	**6**	**H**	**H**	**H**	**D**
P8,12Z	tetradecanedioate (**12**)	**8**	**H**	**H**	**D**	**H**
P10,12Z	tetradecanedioate (**12**)	**10**	**H**	**H**	**D**	**H**
P6,10Z	dodecanedioate (**10**)	**6**	**H**	**H**	**D**	**H**
P6,10XZ	dodecanedioate (**10**)	**6**	**D**	**H**	**D**	**H**
P8,10Z	dodecanedioate (**10**)	**8**	**H**	**H**	**D**	**H**
P10,10Z	dodecanedioate (**10**)	**10**	**H**	**H**	**D**	**H**
P6,4	adipate (**4**)	**6**	**H**	**H**	**H**	**H**
P6,4X	adipate (**4**)	**6**	**D**	**H**	**H**	**H**
P6,4Y	adipate (**4**)	**6**	**H**	**D**	**H**	**H**
P6,4Z	adipate (**4**)	**6**	**H**	**H**	**D**	**H**
P6,4XZ	adipate (**4**)	**6**	**D**	**H**	**D**	**H**
P6,4Q	adipate (**4**)	**6**	**H**	**H**	**H**	**D**

[a] $\boldsymbol{n} = x + 4$.

selectively deuterated liquid crystalline cyanoazobenzene polytetradecanedioates, -dodecanedioates, and -adipates, as investigated by use of FTIR polarization spectroscopy. Furthermore, selected representative members of the different polyester families were investigated by on-line rapid scan FTIR polarization spectroscopy during the laser irradiation. Finally, the fate of the laser-induced anisotropy was similarly investigated by analyzing the anisotropy during heating.

2. Experimental Section

Synthesis of Specifically Deuterated Azobenzene Side-Chain Polyesters. Specifically deuterated precursors and mesogenic monomers, carrying a deuterium content in the labeled positions of more than 93%, were synthesized by using exchange and reduction techniques.[30] Subsequently, a great variety of azobenzene side-chain liquid crystalline polyesters has been prepared by a melt transesterification procedure[31] from the available set of labeled and nonlabeled precursors and monomers based on diphenyl adipate, dodecanedioate, and tetradecanedioate and 2-[ω-[4-[(4-cyanophenyl)azo]phenoxy]-alkyl]-1,3-propanediols. Furthermore, a comprehensive thermal and spectroscopic analysis of all deuterated compounds especially focusing on multinuclei NMR and FTIR spectroscopy was performed. Table 1 provides a survey of the selectively deuterated azobenzene side-chain polyesters under investigation together with the structural formula and the short notation used throughout the paper.

In the notation, the number ***n*** refers to a hexyl ($\boldsymbol{n} = 6$), octyl ($\boldsymbol{n} = 8$), or decyl ($\boldsymbol{n} = 10$) based 2-[ω-[4-[(4-cyanophenyl)azo]-phenoxy]alkyl]-1,3-propanediol, and ***m*** to adipate ($\boldsymbol{m} = 4$), dodecanedioate ($\boldsymbol{m} = 10$), or tetradecanedioate ($\boldsymbol{m} = 12$) based polyesters. **X, Y, Z**, and **Q** designate the deuterated positions in the particular polyester.

Fourier Transform Infrared (FTIR) Polarization Spectroscopy. Samples for infrared measurements were obtained by casting films of the polyesters from chloroform solution (1 mg of polyester/100 μL of solvent) onto pressed KBr pellets positioned on a leveled surface, using a microliter pipet. The films were subsequently dried at room temperature for about 30 min. This preparation procedure results in a film thickness less than 5 μm, which corresponds to a maximum absorbance of approximately 1. In the irradiation experiments, the 488 nm line of an argon ion laser was used. The intensity level of the laser was varied between 300 mW/cm^2 and 1 W/cm^2, and an irradiation time of 100 s for polyadipates (**P6,4**) and 1000 s for polydodecanedioates (**P*n*,10**) and polytetradecanedioates (**P*n*,12**), respectively, was used. The irradiated sample area was adjusted to be 20 mm^2. FTIR polarization spectra of irradiated films were recorded on a Perkin-Elmer 1760X spectrometer with a resolution of 4 cm^{-1}, co-adding 32 scans. Polarization of the infrared beam was obtained using a wire-grid polarizer with ZnSe as substrate. The samples were mounted in the spectrometer in such a way that the polarization of the IR beam could be switched between the parallel (∥) and perpendicular (⊥) direction with respect to the electric field vector of the previously employed argon ion laser beam.

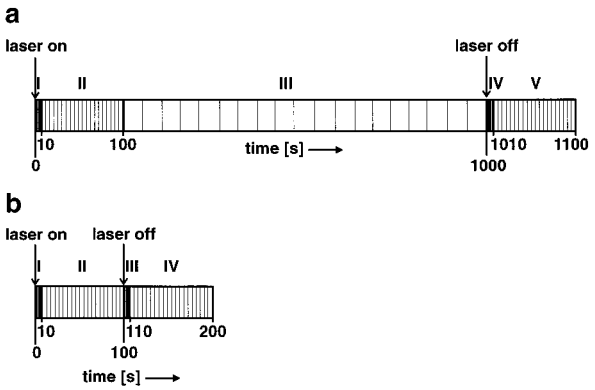

Figure 1. Block representation of the FTIR scanning sequence for an on-line irradiation experiment (a) sequence for **P6,12** systems; (b) sequence for **P6,4** systems.

On-line irradiation experiments and temperature dependent measurements were carried out on polyadipates and -tetradecanedioates in the sample compartment of a Bruker IFS 88 spectrometer. FTIR spectra were recorded simultaneously during laser irradiation with infrared radiation polarized alternately parallel and perpendicular to the incident laser beam polarization with irradiation conditions as above. However, the recording of FTIR polarization spectra continued for another 100 s after the irradiation process. The spectral recording sequences for the on-line experiments are illustrated in Figure 1.

Each sequence contains blocks of polarization spectra (I to V in Figure 1a) recorded during the irradiation process and the subsequent observation period. Each block comprises a distinct number of polarization spectra, accumulating a certain number of scans at a resolution of 4 cm^{-1}. During the first 10 s of irradiation (block I) polarization spectra are taken every second, co-adding 7 scans. The following sequence (block II), ranging form 10 to 100 s, comprises 40 polarization spectra, with a total of 17 scans. In the case of the polytetradecanedioates (**P*n*,12**), irradiation continues for another 900 s. In this interval (block III in Figure 1a) 18 polarization spectra are collected, accumulating 424 scans. After the irradiation process, two additional blocks, equivalent to IV and V, are recorded. Temperature dependent measurements were carried out in a heating cell mounted in the sample compartment. Spectra were recorded at a resolution of 4 cm^{-1} and a total of 32 scans. Starting from 30 °C, the temperature was increased at a rate of 1 °C min^{-1} to a final temperature of 80 °C. Pairs of polarization spectra were taken in a 1 °C interval.

3. Results and Discussion

The transition probability and therefore the observable absorption $\vec{A}$ of a molecular vibration is proportional to $\cos^2(\vec{M}\cdot\vec{E})$, where $\vec{M}$ denotes the transition moment vector of the vibrational mode and $\vec{E}$ the electric

field vector of incident infrared radiation.[32] For an anisotropic oriented sample, the absorption intensity, therefore, depends on the direction of the polarization of the incident infrared radiation. A comparison of the absorption intensities of a particular group vibration for two orthogonal polarized infrared beams will provide a qualitative description of the preferred spatial orientation of this molecular segment. The ratio $R = (A_{\parallel}/A_{\perp})$ of these two intensities is termed the dichroic ratio[32] for the particular absorption band, where the incident infrared radiation is commonly parallel and perpendicular polarized to a given reference direction. This experimentally accessible value might be used to describe the orientational behavior in a quantitative way. Transition moment vectors oriented preferentially perpendicular to the reference direction (σ-dichroism) yield $R < 1$, whereas values $R > 1$ will be obtained for a preferred parallel orientation of $\vec{M}$ (π-dichroism). In the case of uniaxial orientation (verified, e.g., for a nematic phase or uniaxially deformed polymer chains), a quantitative relation[33] between the orientation of a structural group and its dichroic behavior is obtained by evaluating the so-called order parameter S (eq 1), where R_0 denotes

$$S = \frac{(R-1)(R_0+2)}{(R+2)(R_0-1)} \qquad R_0 = \cot^2(\Theta) \qquad (1)$$

the dichroic ratio for perfect axial orientation and Θ the angle between the transition moment $\vec{M}$ and the reference direction. The order parameter S ranges from 0 to 1, indicating isotropic or perfect parallel orientation with respect to the reference direction. However, quantitative as well as qualitative determination of molecular orientation requires a certain knowledge about the direction of the dipole moment change (transition moment) that occurs during the observed group vibration relative to the direction of the particular chemical bonds. Generally, for highly localized vibrations, symmetric and asymmetric CH_2 stretching vibrations, aromatic ring vibrations, and molecular oscillators characterized by a large force constant, e.g., ν(C≡N), the transition moments are fairly well-defined.[32] Each of these group vibrations might therefore serve as an individual molecular probe, monitoring the orientational behavior of the particular functional unit or the related structural segment.

Studies on Irradiated Films. Insight into the orientational behavior of distinct polyester segments can be gained from static FTIR experiments after laser irradiation, by evaluating segment specific group absorptions using polarized infrared radiation. Shortly before performing the laser irradiation experiments, the films were heated to 80 °C in air for 15 min and subsequently rapidly cooled to room temperature in order to destroy possible occurring crystallization effects in long standing films, hence ensuring reproducible starting conditions. Generally, the three polyester families investigated have intricate but different phase behaviors, which will be briefly indicated in the relevant section.

Polytetradecanedioates. The very complex phase behavior of the polytetradecandioates has previously been thoroughly studied,[18,31,34] and the existence of a glass transition in the range 20−25 °C and several ordered phases with transitions between 34 and 72 °C have been established. After rapid cooling from the isotropic melt the lowest, very weak transition at around 34 °C has not been identified whereas a transition at 54 °C is ascribed to a poorly ordered smectic phase.[18,31] However, the coexistence of crystalline domains previously identified as a finely grained texture[18] cannot be excluded in the films.

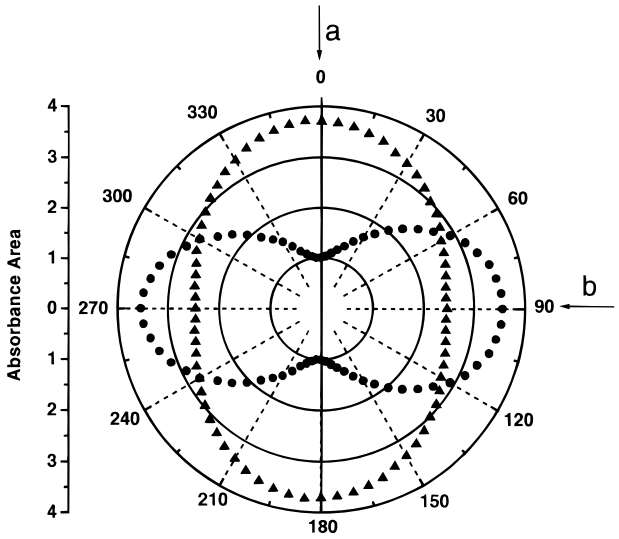

Figure 2. Polar plot of the integrated absorbance area of the aromatic $\nu(C{=}C)_{ring}$ (●, 1601 cm^{-1}) and aliphatic $\nu_s(CD_2)$ (▲, 2091 cm^{-1}) stretching vibration of **P6,12Z** after argon ion laser irradiation (488 nm, 300 mW/cm^2, 1000 s): (←, a) α = 0°, 180° value taken from spectrum in Figure 3a; (←, b) α = 90°, 270° value taken from spectrum in Figure 3b.

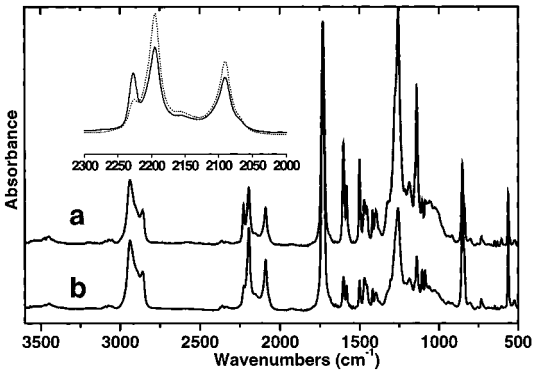

Figure 3. FTIR polarization spectra of **P6,12Z** after argon ion laser irradiation (488 nm, 300 mW/cm^2, 1000 s). The IR radiation is polarized perpendicular (a, —) and parallel (b, ···) to the laser beam polarization.

Figure 2 presents an overlay of polar plots of integrated absorbance areas for the $\nu(C{=}C)_{ar}$ (●) and the $\nu_s(CD_2)$ (▲) stretching vibration of **P6,12Z** after argon ion laser irradiation. Infrared polarization spectra were recorded in 5° intervals; the intersection line between 0 and 180° is parallel to the argon ion laser polarization direction. Figure 3 shows the corresponding FTIR polarization spectra, recorded with IR radiation polarized perpendicular (a) and parallel (b) to the laser polarization.

As previously reported,[35] the strong σ-dichroism observable for the $\nu(C{=}C)_{ar}$ stretching vibrations (1601 + 1582, 1501 cm^{-1}) and the ν(C≡N) absorption at 2228 cm^{-1} emphasize a preferred perpendicular orientation of the azobenzene chromophore with respect to the laser beam polarization direction, as a consequence of light-induced rotational diffusion. Considering the (CD_2) groups specifically located in the aliphatic main-chain spacer, these molecular units serve as an individual

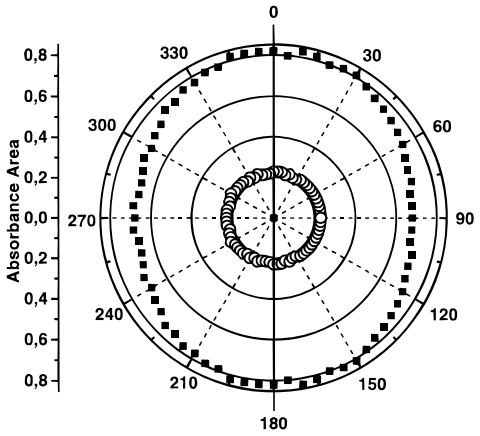

Figure 4. Polar plot of integrated absorbance area of the aliphatic $\nu_s(CD_2)$ (■) stretching vibration of **P6,12Y** and **P6,12X** (○) after argon ion laser irradiation (488 nm, 300 mW/cm^2, 1000 s).

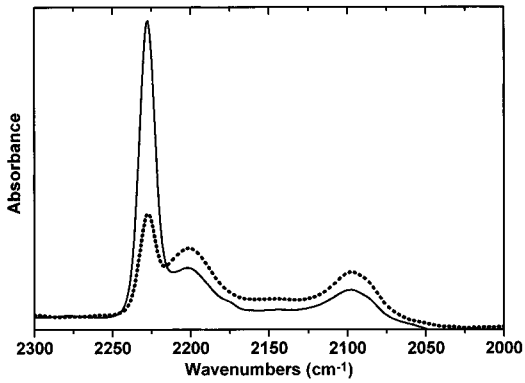

Figure 5. Enlarged FTIR polarization spectra of **P6,12Y** after argon ion laser irradiation (488 nm, 300 mW/cm^2, 1000 s). The IR radiation is polarized perpendicular (—) and parallel (···) to the laser beam polarization.

molecular probe, monitoring backbone alignment.

The change of dipole moment[32] of an oscillating system, equivalent to a (CH_2) or a (CD_2) unit in a $R_1-(CX_2)_n-R_2$ hydrocarbon sequence is perpendicular to the plane of the aliphatic zigzag chain (asymmetric stretching vibration) or perpendicular to the chain axis (symmetric stretching vibration), respectively. The observable π-dichroism for the $\nu_{as}(CD_2)$ and the $\nu_s(CD_2)$ stretching vibrations (2195 and 2091 cm^{-1}) (Figures 2 and 3) indicates, therefore, a preferred perpendicular arrangement of the aliphatic main-chain part relative to the laser polarization.

Due to the fact that the electromagnetic radiation influences initially the orientational behavior of the azobenzene chromophore, the preferred orientation direction of the molecular long axis of this structural unit (the so-called director) has been chosen as the reference direction for the evaluation of the dichroic ratio R. Hence, the dichroic ratio yields a value of $R = 4.04$ for the aromatic stretching vibration and 0.68 for the $\nu_s(CD_2)$ mode (2091 cm^{-1}). Assuming a uniaxial orientational distribution of these polyester segments perpendicular to the argon ion laser polarization direction, the order parameter S for the cyanoazobenzene chromophores—evaluated from the aromatic ring stretching vibrations—yields $S_{(C=C)} = 0.50$, whereas the orientational order of the aliphatic backbone sequence exhibits an order parameter of $S_{(CD_2)} = 0.24$. Following these values as a function of time reveals a slight increase of orientation for the first 3−5 h after the irradiation process, approaching a constant level. Even for the flexible main-chain part, the degree of orientational order remains nearly unchanged for at least 8 months when stored at room temperature.

As already mentioned, quantitative order parameter calculations, using eq 1, require an orientational distribution function, based on uniaxial symmetry. Since such a symmetrical segment distribution might not necessarily be present in photooriented cyanoazobenzene side-chain polyesters, the calculated S values should therefore not be treated as absolute quantities. However, the determination of an order parameter provides a semiquantitative way to correlate and compare laser-induced segmental orientation under the applied experimental conditions for the different cyanoazobenzene side-chain polyester systems.

To examine the orientational behavior of the aliphatic side-chain segments upon irradiation, polyesters (**P6,12Y**) containing a selectively deuterated side-chain spacer have been prepared. According to the synthesis route,[31,32] the two methylene units adjacent to the cyanoazobenzene chromophore as well as the two methylene units next to the side-chain−main-chain link are selectively labeled by deuterium. In the corresponding infrared absorption spectrum, the asymmetric and symmetric $\nu(CD_2)$ stretching vibrations appear at 2200 and 2098 cm^{-1}, respectively. Upon irradiation at 488 nm a weak π-dichroism with respect to the laser beam polarization can be observed for these bands. This is demonstrated by the polar diagram obtained from the integrated absorbance area of the $\nu_s(CD_2)$ stretching vibration (■, Figure 4), as well as the expanded region of corresponding polarization spectra for parallel and perpendicular polarized infrared radiation (Figure 5). This weak dichroic behavior implies a preferred perpendicular arrangement of the aliphatic side-chain spacer with respect to the polarization direction of the incident argon ion laser beam.

However, the dichroic ratio $R = 0.76$, obtained from $\nu_s(CD_2)$, yields an order parameter of $S_{(CD_2)} = 0.17$, indicating that the degree of orientational order for the side-chain spacer is smaller than the main-chain spacer alignment determined above. Furthermore, long-term studies performed at room temperature reveal a decrease of the orientational order for the methylene units in the side-chain spacer after 4 to 5 days, whereas the orientation of the azobenzene moieties, probed by the aromatic ring vibrations, remains unaffected.

It has become evident from the FTIR spectroscopic analyses of all the selectively deuterated polyesters that CH_2 absorptions are more intense in the infrared spectrum than the corresponding CD_2 modes. Thus the $\nu_s(CD_2)$ stretching vibrations of four methylene units (as in Figure 5) exhibit only a relatively weak absorptivity compared to a nondeuterated aliphatic chain of equivalent length. Therefore, it is much more facile to leave only the methylene groups of interest unlabeled in order to determine the absorption behavior of particular methylene units or short aliphatic sequences. This alternative way of characterizing the side-chain spacer orientation has been employed by preparing a thoroughly main-chain labeled polyester, **P6,12XZ**. In addition to the conditions in **P6,12Z**, the four protons of the methylene units in the glycol part (**X**) are replaced by deuterium. Hence, CH_2 absorptions can be entirely attributed to the methylene units of the side-chain

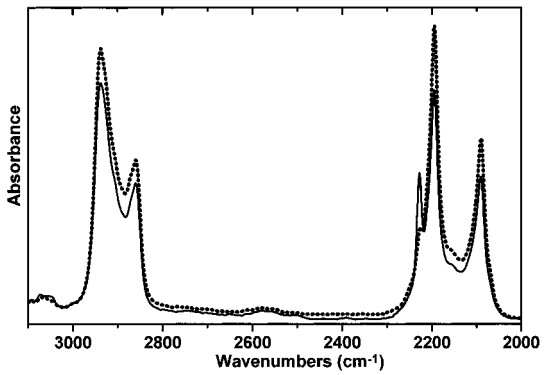

Figure 6. Enlarged FTIR polarization spectra of **P6,12XZ** after argon ion laser irradiation (488 nm, 300 mW/cm^2, 1000 s). The IR radiation is polarized perpendicular (—) and parallel (···) to the laser beam polarization.

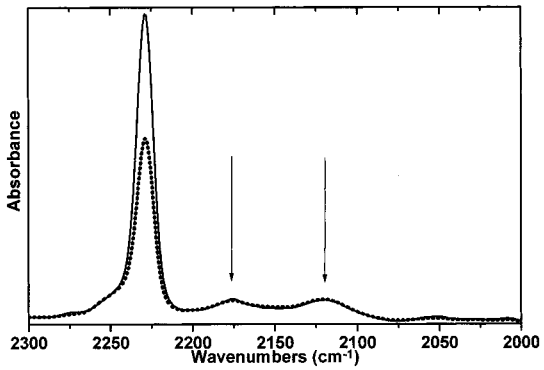

Figure 7. Enlarged FTIR polarization spectra of **P6,12X** after argon ion laser irradiation (488 nm, 300 mW/cm^2, 1000 s). The IR radiation is polarized perpendicular (—) and parallel (···) to the laser beam polarization.

spacer. Figure 6 shows the expanded FTIR polarization spectra of the $\nu(CH_2)$ and $\nu(CD_2)$ absorption region for **P6,12XZ** after irradiation.

The observed dichroism of the $\nu(CH_2)$ stretching vibrations (2938 and 2861 cm^{-1}) emphasizes a perpendicular alignment of the side-chain spacer with respect to the argon ion laser beam polarization. Quantitative evaluations (not shown) are in agreement with the results obtained from the comparable **P6,12Y** system.

A **P6,12X** polyester has been prepared, to determine the orientational behavior of the two methylene units located in the diol part of the polymer main chain. Due to the low number of labeled methylene groups, the intensity of the corresponding $\nu(CD_2)$ infrared absorptions (2176 and 2120 cm^{-1}) is very weak (↓ in Figure 7). Therefore, a reliable quantitative characterization of the orientational behavior based on the infrared dichroism of these bands is not feasible.

However, from the polar diagram obtained from the absorbance area of the $\nu_s(CD_2)$ mode (included in Figure 4, inner circle, ○), no dichroic behavior can be detected. Furthermore, an observable decrease of orientational order reflected by the dichroic ratio determined from the $\nu(CD_2)$ absorptions of **P6,12XZ** in comparison to **P6,12Z**, indicates, at least, no contribution from the methylene groups in the diol part to the perpendicular alignment of the polyester backbone. This result might therefore be interpreted as a local disorder in the vicinity of the main-chain−side-chain junction.

Since laser irradiation has only a direct orientational influence on the azobenzene core, the observed alignment of the aliphatic backbone sequence in the **P6,12** systems might originate from a certain transfer of side-chain anisotropy into the polyester backbone. To study the influence of side-chain spacer length on backbone anisotropy, two cyanoazobenzene side-chain polyesters comprising a perdeuterated aliphatic main-chain spacer together with extended side-chain spacer lengths have been synthesized. An octamethyl (**P8,12Z**) and a decamethyl (**P10,12Z**) sequence should allow for a greater flexibility of the azobenzene chromophore and therefore result in a mechanical decoupling from polyester backbone motion. Irradiation experiments for **P8,12Z** have been carried out under the same conditions applied for **P6,12Z** (488 nm, 300 mW/cm^2, 1000 s), whereas the induction of orientational order in **P10,12Z** requires a higher laser power (1 W/cm^2). Qualitatively, the characteristic segmental group absorptions for all **P*n*,12Z** systems exhibit the same dichroic behavior upon irradiation, indicating equivalent orientational response of the polyester segments. However, as verified in Table 2, variations in side-chain spacer length are reflected in a quantitative manner.

Table 2. Dichroic Ratio (*R*) and Corresponding Order Parameter (*S*) for Selected Group Vibrations of P*n*,12Z Polyesters

	$\nu(C{=}C)_{ring}$		$\nu_s(CD_2)$		$\nu_s(CH_2)^a$	
polyester	*R*	*S*	*R*	*S*	*R*	*S*
P6,12Z[b]	4.04	0.50	0.68	0.24	0.81	0.14
P8,12Z[b]	4.62	0.55	0.63	0.28	0.68	0.24
P10,12Z[c]	7.63	0.69	0.59	0.32	0.62	0.29

[a] Remaining nondeuterated aliphatic methylene groups, characteristic for side-chain spacer orientation. [b] Irradiation at 488 nm, 300 mW/cm^2, 1000 s. [c] Irradiation at 488 nm, 1 W/cm^2, 1000 s.

The data given in Table 2 are illustrative for **P*n*,12Z** polyesters, displaying the largest experimentally achievable dichroism for three distinct vibrational bands. The dichroism of the aromatic $\nu(C{=}C)$ ring stretching vibration monitors chromophore alignment, while the aliphatic $\nu_s(CD_2)$ mode reflects backbone anisotropy. The evaluation of the $\nu_s(CH_2)$ band as a probe for side-chain spacer alignment becomes feasible particularly for octamethyl and decamethyl sequences, since expected interference from the two remaining methylene units in the main-chain diol part might be neglected. Apparently, the order parameter evaluated for the chromophore as well as the aliphatic segments in the main chain and side chain increases gradually while the side-chain spacer length is extended from 6 to 10 methylene units (Table 2). This observable effect is contradictory to an orientational mechanism of the aliphatic main-chain sequences classified as an entirely mechanical coupling process.

Polydodecanedioates. Employing diphenyl dodecanedioate in the polycondensation reaction yields a decamethylene sequence in the polyester backbone. DSC investigations revealed a T_g in both **P6,10** and **P8,10** at 17−18 °C with a large endotherm transition at 35−40 °C for **P6,10** but shifted toward lower temperatures in the case of **P8,10** and actually superposing the T_g. No mesophases were detected and the overall appearance is typical of semicrystalline polymers. In **P10,10**, on the other hand, only a large endothermic (double) peak at 70−80 °C was observed, characteristic of a (highly) crystalline polymer.

The reduction of main-chain spacer length by two methylene units results in response deviations—compared to **P6,12** systems—for the laser-induced alignment

Table 3. Dichroic Ratio (*R*) and Corresponding Order Parameter (*S*) for Selected Group Vibrations of P6,10Z, P6,XZ, and P8,10Z Polyesters Directly after Irradiation and after 20 h

	ν(C=C)$_{ring}$		ν_s(CD$_2$)		ν_s(CH$_2$)	
polyester	*R*	*S*	*R*	*S*	*R*	*S*
P6,10Z[a]	1.20	0.06	0.90	0.07	0.91	0.06
after 20 h	1.97	0.24	0.75	0.18	0.81	0.14
P6,10XZ[b]	1.12	0.04	0.89	0.08	0.97	0.02
after 20 h	2.01	0.25	0.78	0.16	0.83	0.12
P8,10Z[b]	1.12	0.04	0.91	0.06	0.91	0.06
after 20 h	2.14	0.28	0.75	0.18	0.78	0.16

[a] Irradiation at 488 nm, 125 mW/cm^2, 1000 s. [b] Irradiation at 488 nm, 170 mW/cm^2, 1000 s.

process. Table 3 presents dichroic ratios and corresponding order parameter values for **P6,10Z** and **P6,10XZ** systems, evaluated from polarization spectra recorded subsequent to the irradiation process and after annealing the irradiated films at room temperature for 20 h, respectively.

The values given in Table 3 illustrate that infrared polarization spectra recorded shortly after the irradiation process exhibit dichroic ratios close to unity. However, profound photochemical development or reorientation processes are occurring in the dark, leading to a qualitative equivalent orientational arrangement of structural segments, as observed for **P*n*,12** systems. Quantitatively, all polyester segments exhibit a reduced degree of orientational order compared to **P6,12**. Moreover, the **P6,10** systems reveal a more sensitive behavior toward irradiation power in the experimentally available range. A gradual power increase will cause the induced anisotropy to decrease and finally disappear, yielding an isotropic distribution of polyester segments.

The extension of the side-chain spacer to 8 and 10 methylene units, respectively, should again favor a more pronounced decoupling of chromophore and backbone motion. Table 3 likewise contains the dichroic data determined for **P8,10Z**. Obviously, this specimen exhibits the same light-induced dark adaptation for the entire structural segments, as observed for the hexamethylene analogue (**P6,10Z**). However, the required laser power has been found to be slightly higher. In the case of **P10,10Z**, no detectable anisotropy could be induced, using various laser power levels, followed by extended infrared spectroscopic investigations for several days.

Polyadipates. All the investigated polyadipates have T_g from 4 to 12 °C and a smectic A phase melting in the region 53−59 °C depending on the particular deuteration and irrespective of the thermal pretreatment.[31,36]

The reduction of the aliphatic main-chain spacer length to a butylene sequence will lead to close spatial distance between adjacent azobenzene moieties along the polyester backbone, resulting in a reduction of the available free volume and therefore a decrease of segmental flexibility. The reduction of the free volume in **P*n*,4** polyesters, resulting in restricted motional freedom, should also be displayed by differences in the light-induced orientational behavior of polyester segments when compared to **P*n*,10** or **P*n*,12** systems. Figure 8 presents the FTIR polarization spectra of **P6,4Z** recorded after argon ion laser irradiation.

The strong σ-dichroism of the ν(C≡N) vibration (2228 cm^{-1}) in combination with the aromatic ν(C=C) ring

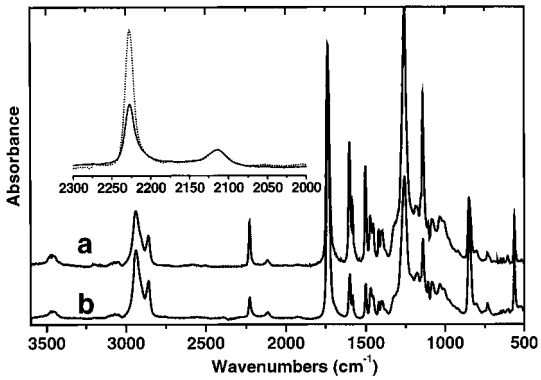

Figure 8. FTIR polarization spectra of **P6,4Z** after argon ion laser irradiation (488 nm, 300 mW/cm^2, 100 s). The IR radiation is polarized perpendicular (a, ···) and parallel (b, —) to the laser beam polarization.

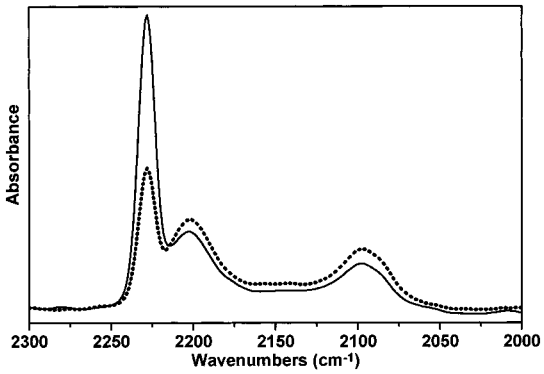

Figure 9. Enlarged FTIR polarization spectra of **P6,4Y** after argon ion laser irradiation (488 nm, 300 mW/cm^2, 100 s). The IR radiation is polarized perpendicular (—) and parallel (···) to the laser beam polarization.

stretching vibrations (1601 + 1582, 1501 cm^{-1}) confirms the expected photoinduced perpendicular alignment of the cyanoazobenzene units with respect to laser beam polarization. The spectral region between 2200 and 2100 cm^{-1} is characterized by a broad absorption band centered around 2115 cm^{-1} and a very weak absorption at 2175 cm^{-1}. As depicted in the spectral enlargement of Figure 8, the absorption at 2115 cm^{-1}, attributable to a ν(CD$_2$) stretching vibration, exhibits no detectable dichroism, indicating no preferred alignment of methylene units in the main-chain spacer after laser irradiation. However, the dichroic ratios determined from the aromatic ring stretching vibrations range between 3.23 and 4.08, which is comparable to chromophore orientation in **P6,12** polyesters. Moreover, the observable dichroism of ν(CH$_2$) absorptions indicates some orientational order for the remaining methylene sequences in the side-chain.

P6,4Y is the diphenyl adipate based equivalent to **P6,12Y**. Thus, information concerning side-chain spacer orientation will be achieved from FTIR dichroic investigations. A comparable weak π-dichroism (R = 0.74) is observed for the ν(CD$_2$) absorptions after irradiation, implying a preferred perpendicular alignment of the aliphatic side-chain sequence with respect to the argon ion laser polarization (Figure 9).

To confirm the results of laser-induced side-chain spacer and main-chain orientation obtained from **P6,4Y** and **P6,4Z**, a thoroughly main-chain deuterated polyester, **P6,4XZ**, has been prepared. In the corresponding infrared spectra, the remaining methylene units located

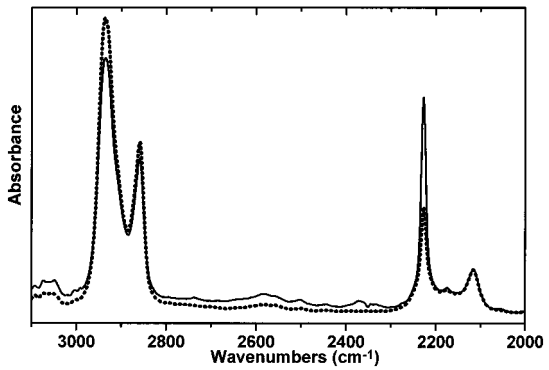

Figure 10. Enlarged FTIR polarization spectra of **P6,4XZ** after argon ion laser irradiation (488 nm, 300 mW/cm^2, 100 s). The IR radiation is polarized perpendicular (—) and parallel (···) to the laser beam polarization.

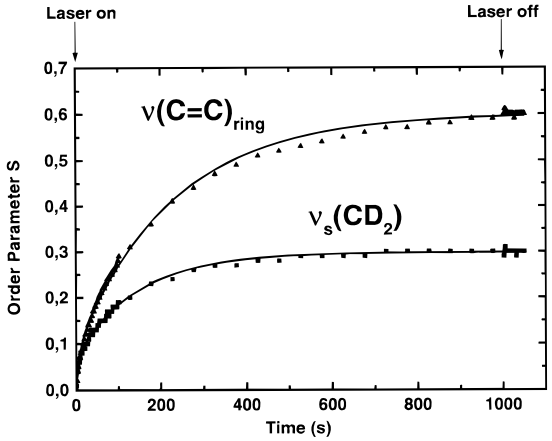

Figure 11. Time dependent segmental orientation of **P6,12Z** monitored by the aromatic ν(C=C)$_{ring}$ and aliphatic ν_s(CD$_2$) stretching vibration during argon ion laser irradiation (488 nm, 300 mW/cm^2).

in the side-chain spacer exclusively contribute to the ν(CH$_2$) absorptions (2935 and 2861 cm^{-1}). Figure 10 presents the enlarged FTIR polarization spectra of **P6,4XZ** recorded after argon ion laser irradiation.

The π-dichroism observed for the ν(CH$_2$) absorptions verifies the preferred perpendicular arrangement of the side-chain spacer relative to the laser polarization. No notable dichroism can be detected for ν(CD$_2$) stretching vibrations (2175 and 2116 cm^{-1}), indicating a random alignment of the polyester backbone. The low infrared absorption intensity of CD$_2$ units selectively located in the diol part of a **P6,4X** polyester prevents an accurate evaluation in terms of orientational order. Hence, no infrared data for **P6,4X** will be presented.

Rapid Scan FTIR Polarization Spectroscopy. Irradiation Experiments. During the irradiation process, the laser-induced molecular alignment has been monitored by rapid scan infrared polarization spectroscopy. Focusing on characteristic group vibrations of polyesters, bearing deuterium atoms in specific molecular positions, allows us to follow the time dependent development of orientational order for different structural segments simultaneously. However, the retarded orientational response observable for **P*n*,10** systems, does not require spectroscopic investigations in the rapid scan mode. Figure 11 presents the time dependent development of orientational order during irradiation, determined from the dichroism of aromatic ν(C=C)$_{ring}$ and aliphatic ν_s(CD$_2$) stretching vibrations in **P6,12Z**.

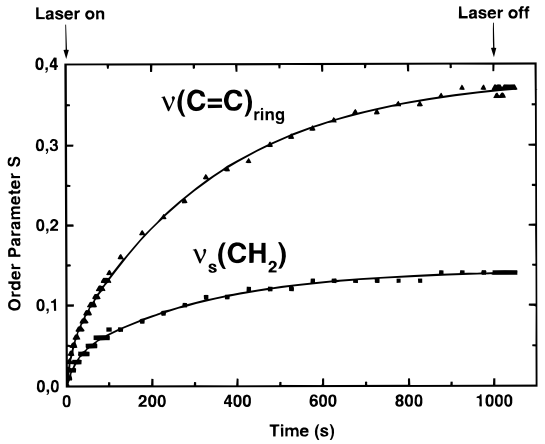

Figure 12. Time dependent segmental orientation of **P6,12XZ** monitored by the aromatic ν(C=C)$_{ring}$ and aliphatic ν_s(CH$_2$) stretching vibration during argon ion laser irradiation (488 nm, 300 mW/cm^2).

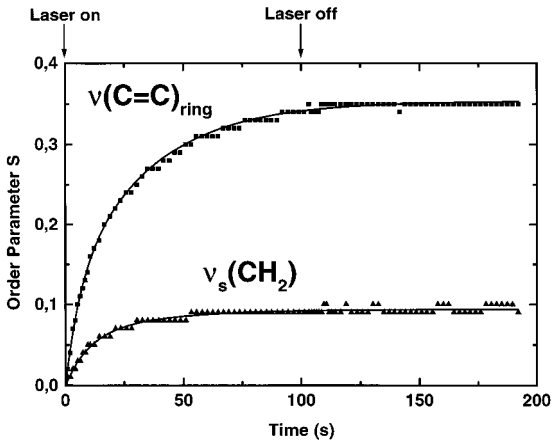

Figure 13. Time dependent segmental orientation of **P6,4Z** monitored by the aromatic ν(C=C)$_{ring}$ and aliphatic ν_s(CH$_2$) stretching vibration during argon ion laser irradiation (488 nm, 300 mW/cm^2).

Since these absorption bands are attributable to group vibrations arising exclusively from the side-chain chromophore and the aliphatic main-chain sequence, respectively, the dichroic behavior monitors the evolution of laser-induced alignment, in particular of these structural segments, as a function of irradiation time. Figures 12 and 13 display the development of orientational order for a **P6,12XZ** and a **P6,4Z** system, respectively. In these cases, the ν_s(CH$_2$) stretching vibration serves as a molecular probe for the aliphatic side-chain spacer alignment.

The shape of the derived order−time correlation can be simulated by fitting the experimentally obtained order parameter values to an associated exponential function[37,38] (eq 2, solid line in Figures 11−13).

$$S = A_1(1 - e^{-k_1 t}) + A_2(1 - e^{-k_2 t}) \qquad (2)$$

This expression (eq 2) implies that the alignment process obeys a first-order kinetics consisting of a fast (index 1) and a slow (index 2) response mode. The parameters k_1 and k_2 display the rate constants of the fast and slow response modes, respectively, whereas A_1 and A_2 are the amplitudes of the particular exponential function. Evaluation of $W_1 = (A_1/(A_1 + A_2))$ and $W_2 = (A_2/(A_1 + A_2))$ indicate, therefore, the weighted contribution of these two processes to the overall alignment.[37]

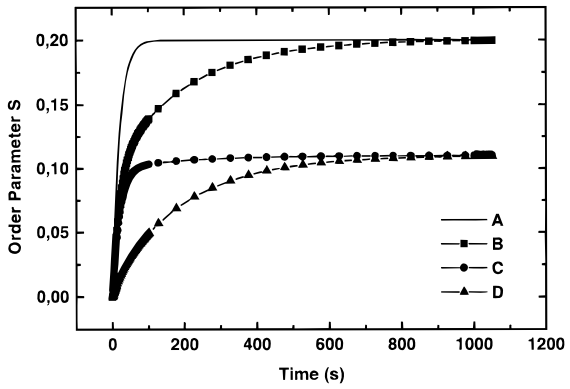

Figure 14. Graphic representation of eq 2 for different parameter combinations A, B, C, D (see Table 4).

Table 4. Differently Simulated Parameter Combinations (Eq 2), Yielding the Order−Time Functions A, B, C, D Displayed in Figure 14

	fast response mode (10^{-2})			slow response mode (10^{-2})		
	A_1	k_1	W_1	A_2	k_2	W_2
A	0.1	5	0.5	0.1	5	0.5
B	0.1	5	0.5	0.1	0.5	0.5
C	0.1	5	0.91	0.01	0.5	0.09
D	0.01	5	0.09	0.1	0.5	0.91

Figure 14 together with Table 4 illustrates the shape of the $S(t)$ function for combinations of different A_i, k_i, and W_i values. Rate constants together with the particular weighted contribution of the fast and the slow response mode influence the slope and the achievable maximum of the order−time function. The significant contribution of the fast response mode to the overall alignment ($W_1 \gg W_2$) yields maximum orientation during a very short time (curve C, Figure 14). Larger W_2 values ($W_2 \geq W_1$), however, indicate a more gradual increase of the order parameter S (curves B and D, Figure 14).

Laser-induced orientation in azobenzene side-chain polyesters generally corresponds to curve D in Figure 14, characterized by the combination of a fast and slow response mode, with a larger contribution of the latter. From Figures 11−13 it becomes apparent that all-polyester structural segments obey the same orientation kinetics and are therefore described by an equivalent mathematical expression. No relaxational effects can be observed either for the chromophore or for the aliphatic side-chain or main-chain segments after the laser has been turned off. The fitted parameters obtained for different structural segments for polyesters based on tetradecanedioic acid (**P6,12**) and adipic acid (**P6,4**) are summarized in Table 5.

For chromophore orientation, the rate constant for the fast response mode k_1 depends on the quantum yield and the rate of isomerization cycles of the azobenzene unit.[37] For aliphatic side-chain spacer alignment, the rate constant k_1 for the fast response mode derived from **P6,12ZX** and **P6,4Z** systems, however, is smaller than the corresponding value for chromophore orientation. This behavior suggests an orientational mechanism for the aliphatic side-chain spacer based on a direct mechanical coupling with the azobenzene chromophore. Though, the corresponding k_2 values, characterizing the slow response mode, are larger for the side-chain spacer orientation compared to the azobenzene unit. Therefore, it has to be assumed that k_2 reflects mainly the local flexibility of the particular segments. After the initial alignment of a small number of segments at the onset of laser irradiation, it is much more facile for additional aliphatic sequences to adopt the anisotropic order by using the accessible volume. Hence, flexible aliphatic sequences reach their maximum achievable order parameter during a relatively short irradiation time. On the other hand, particularly this molecular flexibility of aliphatic segments prevents them from obtaining a high orientational order. Subsequent chain alignment during the irradiation process results in the formation of bent aliphatic sequences caused by spatial restrictions, thus lowering the overall order parameter. Due to the rigid, rodlike structure of the azobenzene chromophores, induction of high orientational order requires a cooperative stacking of the molecular long axis perpendicular to the laser polarization. Therefore, increasing chromophore alignment involves additionally an extensive reorientation of spatial adjacent azobenzene units and aliphatic polyester sequences. The complexity of these processes is reflected in a larger contribution of the slow response mode (W_2), together with smaller k_2 values for chromophore alignment. Remarkably, the aliphatic main-chain spacer in **P6,12** systems responds relatively fast to laser irradiation, resulting in a large k_1 value. This observation, together with the obtained relatively high orientational order of aliphatic main-chain sequences, implies an orientational mechanism different from a simple coupling process solely based on mechanical tension induced by chromophore alignment. It might be assumed that the flexible aliphatic backbone of **P6,12** polyesters regularly folds into the anisotropic matrix structure constituted by the laser-induced chromophore orientation, hereby adopting also a preferred perpendicular alignment with respect to laser polarization. The resulting loss of entropy will be compensated by chain−chain and chain−chromophore interactions of adjacent segments. The proposed mechanism might be similar to the orientational interaction observed for dye-doped low molecular weight liquid crystalline systems.[7]

Polyadipates (**P6,4** systems) exhibit larger k_1 and k_2 values compared to **P6,12** systems. The fast orientational response to laser irradiation can be attributed to the purely liquid crystalline phase behavior of these systems. The mesophases—inherent for **P6,4** systems—exhibit a larger intrinsic mobility compared to the semicrystalline multiphase structure observable for **P6,12** polyesters.

Temperature Dependent Measurements. Erasure of photoinduced anisotropy in polyester films is accomplished by heating the films into the isotropic phase. The isotropization temperature has been determined by differential scanning calorimetry.[31] In the case of **P6,12** polyesters, this temperature varies for the differently labeled systems between 67.6 and 71.9 °C. To study the temperature dependent disappearance of photoinduced segmental alignment, the heating process has been simultaneously followed by infrared polarization spectroscopy. The decline and final vanishing of infrared dichroism for individual absorption bands indicate the transformation toward isotropic distribution of the particular polyester segment. Figure 15 shows both the differential scanning trace together with the order parameter calculated from the dichroic ratio of the aromatic ring stretching vibration ($\nu(C{=}C)_{ring}$) and the $\nu_s(CD_2)$ stretching vibration for **P6,12Z**, over a temperature range between 30 and 80 °C.

Table 5. Fitted Parameters (Eq 2) for Experimentally Derived Order−Time Relations for Different Polyester Segments

		fast response mode (10^{-2})			slow response mode (10^{-2})		
polyester	segment	A_1	k_1	W_1	A_2	k_2	W_2
P6,12Z	chromophore	0.084	12.759	0.140	0.517	0.446	0.860
	main chain	0.074	14.225	0.247	0.225	0.681	0.753
P6,12XZ	chromophore	0.048	7.505	0.124	0.337	0.291	0.876
	side chain	0.034	4.479	0.236	0.109	0.328	0.764
P6,4Z	chromophore	0.110	15.967	0.312	0.243	2.897	0.688
	side chain	0.046	11.781	0.488	0.048	3.413	0.512

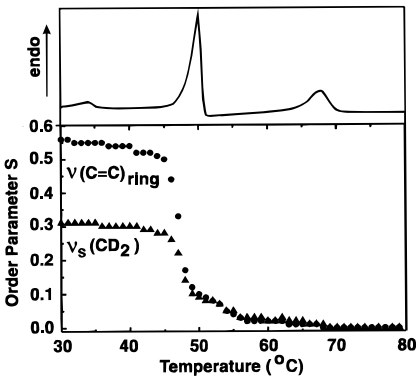

Figure 15. DSC trace and temperature dependent disappearance of orientational order for chromophore and backbone orientation of **P6,12Z** monitored by the aromatic $\nu(C{=}C)_{ring}$ and aliphatic main chain $\nu_s(CD_2)$ stretching vibration (heating rate: 1 °C/min).

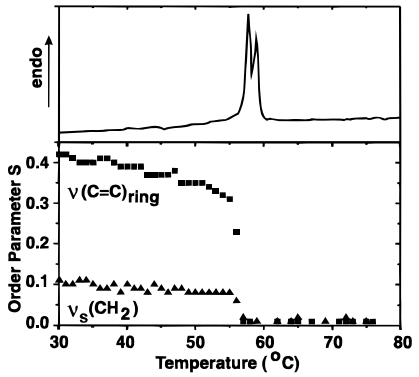

Figure 16. DSC trace and temperature dependent disappearance of orientational order for chromophore and side-chain spacer orientation of **P6,4Z** monitored by the aromatic $\nu(C{=}C)_{ring}$ and aliphatic $\nu_s(CH_2)$ stretching vibration (heating rate: 1 °C/min).

Obviously, the temperature dependent disappearance of laser-induced orientational order in thin polyester films is primarily controlled by the thermal behavior of the polyester bulk sample. The $S(T)$ function between 30 and 45 °C exhibits for both segments an almost linear shape, followed by a sharp decrease, corresponding to a profound endotherm phase transition at $T_{peak} = 49.8$ °C observable in the DSC trace. Most of the induced alignment of azobenzene chromophores and aliphatic main-chain segments is lost over a narrow temperature interval of $\Delta T = 5$ °C. The remaining orientational order decreases continuously with increasing temperature and is completely lost when the endothermic phase transition at $T_{peak} = 67.6$ °C is exceeded. Equivalent behavior can be found for the temperature dependent disappearance of aliphatic side-chain spacer alignment in **P6,12XZ** systems. Extending the side-chain spacer length to an octa- and decamethylene sequence favors crystalline aggregation in the polyester bulk sample, resulting in one broad endothermic phase transition, exhibiting a larger heat of fusion at comparable higher temperatures (**P8,12Z** $T_{peak} = 60$ °C, **P10,12Z** $T_{peak} = 70$ °C). According to the shift of transition temperatures, the photoinduced segmental orientation in **P8,12Z** and **P10,12Z** polyesters is preserved over a wider temperature range. In both cases main-chain and side-chain alignment vanishes instantaneously in a temperature interval of $\Delta T = 10$ °C. The thermal behavior of **P6,4** systems is characterized by two liquid crystalline phase transitions at 58 and 59 °C, respectively.[31] Figure 16 comprises the DSC trace and calculated S(T) values from aromatic ring and aliphatic $\nu(CH_2)$ stretching vibrations of a **P6,4XZ** polyester.

Apparently, the aliphatic side-chain spacer and chromophore orientation disappear simultaneously while approaching the first endothermic phase transition at 58 °C.

4. Conclusion

If one considers a "photoinduced rotational diffusion" as the basic mechanism for the alignment process of the azobenzene chromophores, the molecular long axis should be randomly aligned in the *X*,*Y*-plane perpendicular to the laser polarization direction. In this conformation, the transition moment exhibits no component in the electric field vector direction and hence the transition probability vanishes. As previously described for **P6,12** polyesters[18] and generally confirmed for **P*n*,12**, **P*n*,10**, and **P6,4** systems, the experimentally observed dichroic behavior originating from characteristic chromophore vibrations confirms a photoinduced preferred perpendicular alignment of the molecular long axis with respect to the polarization direction of the incident argon ion laser beam. The induced macroscopic anisotropy is permanently preserved, upon storing the polyester films at room temperature, despite the glass transition for all systems being below 25 °C.[31] Irradiation experiments performed on a selectively labeled specimen reveal that in favorable cases photoinduced chromophore alignment has additionally a remarkable orientational influence on the remaining polyester segments. Individual group absorptions, characteristic of distinct aliphatic side-chain and main-chain sequences exhibit a weak to medium infrared dichroism, indicating a transfer of anisotropy into the macromolecular structure. Figure 17 presents a schematic representation (top view) of the laser-induced segmental orientation in **P*n*,12** and **P*n*,10** systems as derived from the FTIR dichroic investigations. According to the observed dichroic behavior of selected group vibrations, all polyester segments should be preferentially aligned in the *X*,*Y*-plane of the polyester film. Since the orientational information obtained from the described infrared polarization experiments is solely restricted to the *Y* and *Z* direction (polarization direction of the infrared beam), no prediction can be made about the local segmental order in the *X*,*Y*-plane. However, assuming a statistical

Table 6. Qualitative Relations between Film Morphology, Laser Response and Induced Orientation at Ambient Temperature of Different Polyester Systems

polyester	morphology	laser response	induced orientation
P6,4	completely mesomorphic	fast	low
Pn,12	coexistence of mesomorphic and crystallinne domains	moderate	large
Pn,10	semi- crystalline or crystalline	retarded	low to no orientation at all

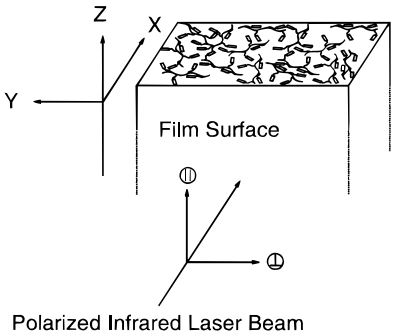

Figure 17. Schematic presentation of the laser-induced segmental orientation in **P*n*,12** and **P*n*,10** polyesters as derived from FTIR dichroic investigations of selectively labeled systems.

process as basis for the light-induced chromophore orientation, a random conformation in the *X*,*Y*-plane has to be assumed.

Rapid-scan FTIR polarization experiments illustrate that alignment of aliphatic segments arises simultaneously with chromophore orientation. The smaller rate constant k_1 observed for the aliphatic side-chain spacer alignment indicates that anisotropy is induced by mechanical tension based on the orientation of azobenzene chromophores. The large value obtained for the rate constant k_1 for backbone alignment in **P6,12** systems together with the relatively high order parameter calculated for backbone alignment in **P6,12** polyesters might be attributed to a matrix-assisted orientational effect. It has to be assumed that the anisotropic matrix created by the azobenzene chromophores serves as an orientation pattern for the flexible aliphatic main-chain sequence.

No relaxation of backbone anisotropy can be detected after the irradiation process, illustrating a physical stability of the photoinduced conformation. This stability might be due to aggregational effects or further crystallization processes. However, recent atomic force microscopic investigations[39,40] carried out on **P6,12** systems have shown that laser-induced optical anisotropy is accompanied by the macroscopic appearance of a topographic grating structure followed by a pronounced increase of surface roughness after a period of about 4 h. The subsequent development of surface structure can be attributed to a recrystallization of polyester segments. This process of "photo-induced" main-chain aggregation might be compared to the formation of spherulitic structures. The tendency to form associated structures of parallel ordered chains has also been described for various polymers[41] cooled rapidly from the melt.

The correlation between the isotropization temperature of laser-induced orientation in thin polyester films, determined by temperature dependent infrared investigations, and the appearance of endothermic bulk phase transitions, characterized by DSC, directly relates the preservation of photoinduced anisotropy to the morphological phase behavior. Apparently, aggregation tendency and crystallization require a certain degree of backbone flexibility. Due to the short aliphatic main-chain sequence and therefore close spatial spacing between adjacent side-chain azobenzene moieties, polyadipates exhibit only restricted motional freedom. Hence, chromophore alignment is not accompanied by a macroscopic backbone anisotropy. Stabilization of the photoinduced chromophore orientation will only be achieved by dispersive interactions between the aligned azobenzene units. Since the laser-induced macroscopic chromophore orientation in the **P6,4** systems vanishes at the nematic−isotropic phase transition, it has to be assumed that the mono domain created by laser-induced orientation of azobenzene moieties reflects the arrangement of these mesogens in the corresponding nematic poly domain structure.

The experimentally observed response times and quantities of orientational order, characterized by the order parameter, can be related to the existent morphology of the particular polyester system. These facts are summarized in Table 6.

Since it has previously been shown experimentally[24] that laser irradiation has no significant influence on the temperature of the irradiated polyester films, the heat transfer during exposure is not sufficient to destroy crystalline aggregates. Formation of crystalline structures with high transition temperatures, as achieved during the annealing processes of **P*n*,12** systems,[18,20,34] indeed prevent the introduction of orientational order by laser irradiation. Hence, it has to be assumed that the alignment process is not based on a thermal transformation of the system into the isotropic melt and subsequently freezing in the orientational order by quenching the films after turning off the laser beam. It is rather the existence of mesomorphic domains, characterized by a large intrinsic mobility, which is essential for inducing orientational effects. However, the ability to form crystalline structures is necessary for the preservation of anisotropic order.

Acknowledgment. C.K., S.H., and P.S.R. (Risø National Laboratory) gratefully acknowledge the financial support for this research from the Danish Polymer Centre supported by the Danish Materials Technology Development Program (MUP2). C.H. and H.W.S. (University of Essen) extend their thanks to the Brite/EuRam Program under contract BRE2.CT93.0449.

References and Notes

(1) Roth, J. P. *Rewritable Optical Storage Technology*; Meckler: Westport, London, U.K., 1991
(2) Kryder, M. H. *Annu. Rev. Mater. Sci.* **1993**, *23*, 411
(3) McArdle, C. B., Ed. In *Side Chain Liquid Crystal Polymers*; Blackie and Son Ltd.: Glasgow, U.K., 1989, Chapter 13, pp 357−394 (and cited literature).
(4) Chilton, J. A., Gossey, M. T., Eds. *Special Polymers for Electronic and Optoelectronics*; Chapman & Hall: London, U.K., 1995.
(5) Psaltis, D.; Mok, F. *Sci. Am.* **1995**, 52.
(6) Rau, H. In *Photochemistry and Photophysics*; Rabek, J. F., Ed.; CRC Press: Boca Raton, FL, 1990; Vol. II, Chapter 4, p 119.
(7) Gibbons, W. M.; Shannon, P. J.; Sun, S.-T.; Swetlin, B. J. *Nature* **1991**, *351*, 49.

(8) Chen, A. G.; Brady, D. J. *Opt. Lett.* **1992**, *17*, 441.
(9) Natansohn, A.; Rochon, P.; Gosselin, J.; Xie, S. *Macromolecules* **1992**, *25*, 2268.
(10) Xie, S.; Natansohn, A.; Rochon, P. *Chem. Mater.* **1993**, *5*, 403.
(11) Berg, R. H.; Hvilsted, S.; Ramanujam, P. S. *Nature* **1996** *383*, 505
(12) Eich, M.; Wendorff, J. H.; Reck, B.; Ringsdorf, H. *Makromol. Chem., Rapid Commun.* **1987**, *8*, 59.
(13) Anderle, K.; Birenheide, R.; Eich, M.; Wendorff, J. H. *Makromol. Chem., Rapid Commun.* **1989**, *10*, 477.
(14) Wiesner, U.; Antonietti, M.; Boeffel, C.; Spiess, H. W. *Makromol. Chem.* **1990**, *191*, 2133.
(15) Stumpe, J.; Muller, L.; Kreysig, D. *Makromol. Chem., Rapid Commun.* **1991**, *12*, 81.
(16) Haitjema, H. J.; von Morgen, G. L.; Tan, Y. Y.; Challa, G. *Macromolecules* **1994**, *27*, 6201.
(17) Hvilsted, S.; Andruzzi, F.; Ramanujam, P. S. *Opt. Lett.* **1992**, *17*, 1234.
(18) Hvilsted, S.; Andruzzi, F.; Kulinna, C.; Siesler, H. W.; Ramanujam, P. S. *Macromolecules* **1995**, *28*, 2172.
(19) Ramanujam, P. S.; Holme, N. C. R.; Nikolova, L.; Berg, R. H.; Hvilsted, S.; Kristensen, E. T.; Kulinna, C.; Nielsen, A. B.; Pedersen, M. In *Practical Holography XI and Holographic Materials III*; Benton, S. A., Torut, T. J., Eds.; *Proceedings of SPIE* No. 3011; SPIE: Bellingham, WA, 1997; p 319.
(20) Ramanujam, P. S.; Holme, C.; Hvilsted, S.; Pedersen, M.; Andruzzi, F.; Paci, M.; Tassi, E. L.; Magagnini, P. L.; Hoffman, U.; Zebger, I.; Siesler, H. W. *Polym. Adv. Technol.* **1996**, *7*, 768.
(21) Holme, N. C. R.; Ramanujam, P. S.; Hvilsted, S. *Opt. Lett.* **1996**, *21*, 902.
(22) Kulinna, C.; Zebger, I.; Hvilsted, S.; Ramanujam, P. S.; Siesler, H. W. *Macromol. Symp.* **1994**, *83*, 169.
(23) Ramanujam, P. S.; Hvilsted, S.; Zebger, I.; Siesler, H. W. *Macromol. Rapid Commun.* **1995**, *16*, 455.
(24) Holme, N. C. R.; Ramanujam, P. S.; Hvilsted, S. *Appl. Opt.* **1996**, *35*, 4622.
(25) Ramanujam, P. S.; Hvilsted, S.; Andruzzi, F. *Opt. Rev.* **1994**, *1*, 30.
(26) Ramanujam, P. S.; Hvilsted, S.; Andruzzi, F. *Appl. Phys. Lett.* **1993**, *62*, 1041.
(27) Ramanujam, P. S.; Hvilsted, S.; Andruzzi, F.; Kulinna, C.; Siesler, H. W. In *Organic Thin Films for Photonic Applications*; Technical Digest Series Vol. 17; Optical Society of America: Washington, DC, 1993; p 244.
(28) Spiess, H. W. *J. Chem. Phys.* **1980**, *72*, 6755.
(29) Spiess, H. W. *Pure Appl. Chem.* **1985**, *57*, 1617.
(30) Hendann, C.; Siesler, H. W.; Andruzzi, F.; Kulinna, C.; Hvilsted, S. *Mol. Cryst. Liq.* Cryst., in press.
(31) Kulinna, C.; Hvilsted, S.; Hendann, C.; Siesler, H. W.; Andruzzi, F. *Mol. Cryst. Liq.* Cryst., in press.
(32) Zbinden, R., Ed. *Infrared Spectroscopy of High Polymers*; Academic Press: New York, 1964.
(33) Neff, V. D. In *Liquid Crystal and Plastic Crystal*; Gray, G. W., Winsor, P. A., Eds.; John Wiley & Sons: New York, 1975; p 231.
(34) Tassi, E.; Paci, M.; Magagnini, P. L. *Mol. Cryst. Liq. Cryst.* **1995**, *266*, 135.
(35) Zebger, I.; Kulinna, C.; Siesler, H. W.; Andruzzi, F.; Pedersen, M.; Ramanujam, P. S.; Hvilsted, S. *Macromol. Symp.* **1995**, *94*, 159.
(36) Kulinna, C.; Zebger, I.; Hvilsted, S.; Ramanujam, P. S.; Siesler, H. W., *Macromol. Symp.* **1994**, *83*, 169.
(37) Ho, M. S.; Natansohn, A.; Rochon, P. *Macromolecules* **1995**, *28*, 6124.
(38) Buffeteau, T.; Pézolett, M. *Appl. Spectrosc.* **1996**, *50*, 948.
(39) Ramanujam, P. S.; Holme, N. C. R.; Hvilsted, S. *Appl. Phys. Lett.* **1996**, *68*, 1329.
(40) Holme, N. C. R.; Nikolova, L.; Ramanujam, P. S.; Hvilsted, S. *Appl. Phys. Lett.* **1997**, *70*, 1518.
(41) Thinius, K. *Plaste Kautschuk* **1971**, *18*, 408.

MA970967W